Supplement 2: Benthic flume calibration

Bed Shear Stress Calculation for Voyager II (large flume, far-field surveys)

Bed shear stress is the parameter which is most commonly used in issues of sediment transport. (Time-averaged) flow velocity (0.13 m above the bed) data (*u, v, w,* m s^{-1}) (in conjunction with applied voltage – paddle rotation rate, Ω data) were collected within the annular flume under clear-water conditions over a roughened polystyrene artificial bed. These were filtered for quality following procedures recommended by Nortek. Data with a signal to noise ratio (SNR) lower than 15 and/or a correlation less than 85% were discarded. Mean shear velocity ($\bar{u}_*$, m s^{-1}) was calculated from the (mean) flow velocity measurements ($\bar{u}$) using the following empirical relationship (obtained from collaborative calibration studies by Partrac and NOCS):

$$\bar{u}_* = 0.0167 + 0.097\bar{u}, \text{ m s}^{-1}$$

This equation is valid over a full operating range of current speeds. The corresponding value for bed shear stress was derived using the expression

$$\tau_o = \rho\bar{u}_*^2$$

Because the shear velocity / bed stress calibration was derived from clear water studies, and it is known that the presence of sediment in suspension can feedback and reduce bed stress (so-called 'drag reduction') it is necessary to correct for the evolution of high suspended sediment concentrations during erosion runs. The change in bed stress u_{*s} is a function both of the sediment concentration and the bed stress imposed by paddle rotation, and was derived by Amos et al., (1992b):

$$u_{*s} = u_* - (0.2267\left[log_{10}S\right]\left\{\frac{u_*}{6.35}\right\}), \text{ m s}^{-1}$$

Bed Shear Stress Calculation for Voyager I (mini flume, near-field surveys)

A flow calibration exercise was performed using a) a laser-PIV system and b) the Nortek ADV 3D point sensor. The laser PIV system provided detailed, mean sectional azimuthal and resultant flow velocity @ 0.05 m above the bed, which is useful given the ultra-high resolution and 2D areal coverage of the flume, whereas the ADV sensor provided high temporal resolution data which can be processed to provide an estimate of bed stress. The measurement volume of the ADV was 1-2 mm above the flume artificial bed (a roughened polystyrene foam).

A 2-D Dantec Flow Map PIV system was utilized to determine the detailed flow velocity field within the flume annulus. The PIV method measures the horizontal azimuthal (U_θ) and radial velocity (U_r) fields at a given height above the bed in great spatial detail within the annulus. A major advantage of this measurement technique is that it is non-intrusive and it provides a synoptic map of velocity fields at any chosen elevation within the fluid disturbance field. The technique employs a double-pulsed laser light source, suitably aligned to generate a light sheet at any plane within the flow. In the present experiments, the axis of the flume was vertical and the light sheet was adjusted to be horizontal, illuminating the flow at a prescribed, constant elevation level in the fluid. To avoid problems with limitations of the field of view of the optical components of the PIV system and to

exploit the symmetrical property of the flume system, a measurement area incorporating one-quarter of the total annular channel plan area was chosen. A CCD camera and 45° mirror arrangement was employed to record velocity field data from below the channel for a duration of 30 s at each predetermined elapsed time after initiation of the paddle motion. To optimise the PIV system the seawater within the channel was initially seeded with Iriodin 100 (Silver Pearl) tracer particles. Calibration grids were placed at the prescribed elevations prior to an experimental run, thereafter being removed before the paddle forcing was initiated.

Post-processing and analysis of the recorded flow fields was carried out using the Flow Manager 3D-PIV software package (used in 2-D mode) and data generated are presented in a polar coordinate field (i.e. x-y co-ordinates are references to the axis of rotation).

Experimental runs were carried out for four different flume depths(H= 0.20m, 0.25 m, 0.30 m, 0.34 m), in which for each case, the lid rotation (paddle) rate Ω was increased incrementally by $\Delta_\Omega = 2$ from 0 to 30 cm s^{-1} (as in field tests). In these runs, the duration t_{acc} of the linear acceleration ramp process was 60 s and the time interval Δt_e was fixed at 300 s; for each increase in paddle speed, measurements of the fluid velocity field were taken continuously for an interval of 30 s, starting at 240 s after the end of the ramping process (i.e. 240 s from the start of each constant paddle speed phase).

An example of the filtered data output showing the spatial distribution of flow vectors is given in Figure S1. The velocity data represent time-averaged values of horizontal velocity over the 30 s acquisition interval.

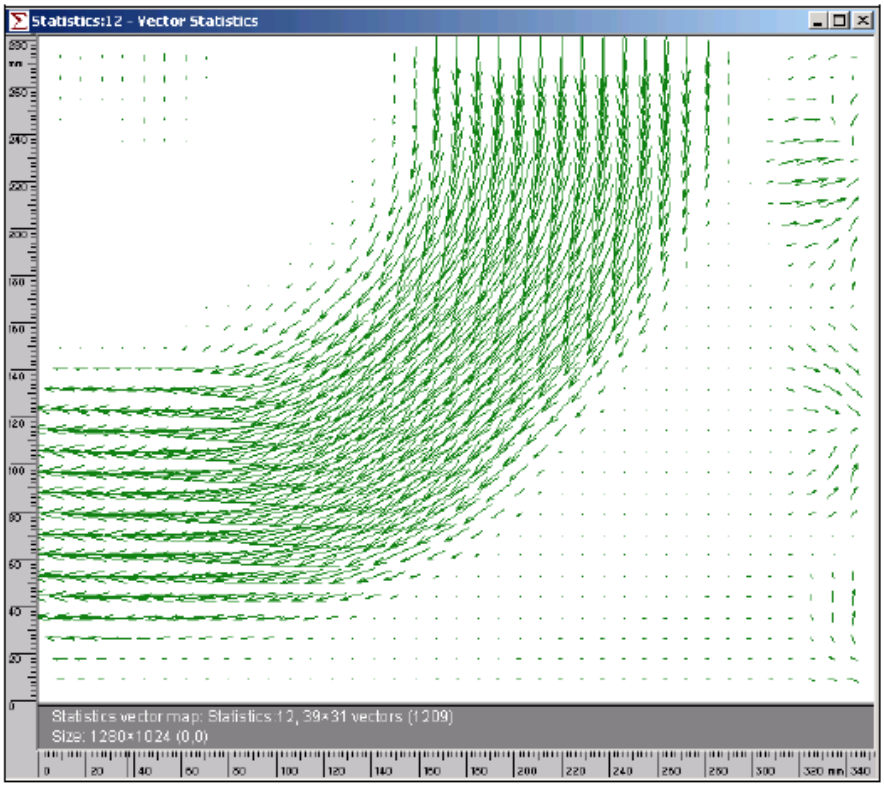

Figure S1. Illustrative vector map (statistical temporal average) for a single velocity (paddle rotation rate) setting.

The PIV method measures the horizontal azimuthal (U_θ) and radial velocity (U_r) fields; the resultant horizontal velocity at any point is given by $U_R^2 = U_r^2 + U_\theta^2$ and the horizontal sectional average value

($U_{R,ave}$) is calculated as $\Sigma U_R/n$ where n is the number of data points along a flow transverse transect from the inner to the outer wall. $U_{R,ave}$ is the velocity metric of interest to the use of the flume in this study.

From this data, relationships between the rotation rate Ω of the paddles (i.e. lid rotation rate) through an erosion test and $U_{R,ave}$ for each of the four values of channel depth (H) were formed. Table S1

summarises the relationship between these two variables following linear least squares regression analysis of the raw data. These equations can thus be used to transform field measurements of Ω into channel flow velocities.

Table S1: Summary of the predictive equations derived from least squares regression analysis of flow calibration data.

H (cm)	Regression equation	r^2
35	$U_{R,ave} = 0.0081\Omega - 0.0109$	0.99
30	$U_{R,ave} = 0.0079\Omega - 0.0186$	0.99
25	$U_{R,ave} = 0.0071\Omega - 0.0175$	0.99
20	$U_{R,ave} = 0.0067\Omega - 0.094$	0.98

For each of the sediment to lid distances (H) used in the field (H=15, 20, 25 cm only) the lid rotation frequency Bed stress (τ_o), for each velocity time-step/ lid rotation (paddle) rate Ω, was computed directly from PIV time-series flow data and using the TKE methodology (Widdows et al., 2006) using a proportionality constant C1 of 0.19 (after Soulsby, 1983; Stapleton and Huntley, 1995; Thompson et al., 2003). The veracity of estimates of bed stress were also double checked on 3 occasions using visual observations of the entrainment of uni-modal abiotic sand within the flume (*d50* 200 μm; 400 μm; 1 mm). Finally, the drag reduction expression of Amos et al., (1992b) (see above) was applied to the stress time series to account for stress reduction due to evolving high sediment concentrations.

Turbidity Sensor Calibrations

The on-board OBS (turbidity) sensors record raw data as a voltage; this requires conversion into scientific (sediment concentration) units (here mg l^{-1}). A series of calibrations was undertaken using surface scrapes (upper 1 cm) from bottom sediment samples collected at each site using a van Veen grab. Samples were collected, bagged and frozen during both surveys (photographs of each grab were taken (see Appendix I). For each calibration concentration reference standards were made by mixing a known dry mass of sediment into a known volume of seawater. Eight standards were made up for each site. The OBS sensor was sequentially exposed to these suspensions, and least-squares regression analysis (Fowler et al., 1989) used to generate an equation relating sensor voltage to sediment concentration. Table S2 summarises the regression equation for each site from the Far-Field survey and Table S3 from the Near-Field survey.

Table S2. Summary of regression equations from the turbidity sensor calibrations (y=concentration, mg l^{-1}, x=instrument readout) for the far-field (FF) survey.

Site Name	Equation	r^2
Bloody Bay 1	y = 0.0463x – 1.4577	0.95
Bloody Bay 2	y = 0.0450x + 0.1689	0.95
Fiunary 1	y = 0.1844x – 13.0195	0.95
Fiunary 2	y = 0.1640x – 11.0471	0.85
Shuna Castle Bay 1	y = 0.0427x + 9.8368	0.74
Shuna castle Bay 2	y = 0.1055x – 2.7369	0.98
BDNC 1	y = 0.0489x + 0.2655	0.93
BDNC 2	y = 0.0785x – 2.9269	0.93
Ardfuir 1	y = 0.1338x – 5.7198	0.88
Ardfuir 2	y = 0.0729x – 0.7424	0.97
Port na Moine 1	y = 0.0153x + 3.6996	0.67
Port na Moine 2	y = 0.1026x – 2.0047	0.98
Durmyon Bay 1	y = 0.1349x – 4.1568	0.96
Durmyon Bay 2	y = 0.1203x – 1.2797	0.99

Table S3 Summary of regression equations from the turbidity sensor calibrations (y=concentration, mg l^{-1}, x = instrument readout) for the near-field survey.

Site Name	Equation	r^2
BDNC001	$y = 2.0121x - 46.64$	0.97
BDNC002	$y = 2.1749x - 17.75$	0.98
BDNC003	$y = 1.9543x + 0.0462$	0.99
Dunstaffnage 001	$y = 1.5146x - 29.7022$	0.96
Dunstaffnage 002	$y = 1.9612x - 36.1864$	0.91
Dunstaffnage 003	$y = 1.2575x + 3.8008$	0.83
Port na Gillie 001	$y = 2.3027x - 85.8541$	0.96
Port na Gillie 002	$y = 2.1808x - 37.2986$	0.99
Port na Moine 001	$y = 0.8945x + 38.2554$	0.71
Port na Moine 002	$y = 2.3857x - 24.4069$	0.90
Scallastle Bay 002	$y = 1.2128x - 36.2136$	0.88
Scallastle Bay 001	$y = 1.5521x - 9.4223$	0.98
Shuna Castle Bay 002	$y = 2.0381x - 31.1336$	0.99
Shuna Castle Bay 001B	$y = 1.4320x + 11.9877$	0.96